Direct observation of twin domains of NiO(100) by x-ray linear dichroism at the O *K* edge using photoemission electron microscopy

Kuniaki Arai,[1] Taichi Okuda,[2,*] Arata Tanaka,[3] Masato Kotsugi,[4,5] Keiki Fukumoto,[4] Takuo Ohkochi,[4] Fangzhun Guo,[4] Tetsuya Nakamura,[4] Tomohiro Matsushita,[4] Takayuki Muro,[4] Masaki Oura,[6] Yasunori Senba,[4] Haruhiko Ohashi,[4] Akito Kakizaki,[1] and Toyohiko Kinoshita[4,5]

[1]*The Institute for Solid State Physics, The University of Tokyo, Kashiwanoha 5-1-5, Kashiwa, Chiba 277-8581, Japan*
[2]*Hiroshima Synchrotron Radiation Center, Hiroshima University, Kagamiyama 2-313, Higashi-Hiroshima, Hiroshima 739-0046, Japan*
[3]*Department of Quantum Matter, ADSM, Hiroshima University, Higashi-Hiroshima, Hiroshima 739-8530, Japan*
[4]*Japan Synchrotron Radiation Research Institute, Sayo, Hyogo 679-5198, Japan*
[5]*CREST-JST, Kawaguchi, Saitama 332-0012, Japan*
[6]*RIKEN SPring-8 Center, Sayo, Hyogo 679-5148, Japan*

(Received 13 September 2011; revised manuscript received 18 January 2012; published 1 May 2012)

The domain structure of antiferromagnetic (AFM) NiO(100) has been investigated by nonmagnetic x-ray linear dichroism (XLD) at the O *K* edge using photoemission electron microscopy and linearly polarized x-ray light. The evolution of XLD image contrast as the function of the angle between the crystal orientation and the incident *s*- or *p*-polarized light is clearly observed. The angular dependence of the XLD contrast is in good agreement with the calculated x-ray absorption cross section of O 1*s* to 2*p* orbital that is deformed anisotropically by the strong hybridization with Ni 3*d* orbitals. This agreement strongly supports the conclusion that the observed XLD contrast reflects the twin-domain (*T*-domain) structure of the NiO crystal. By comparing the experimental data with the calculation, it is possible to assign each domain contrast to a specific *T*-domain in the quantitative manner. The proposed simple and clear way of *T*-domain assignment will be useful for investigating the magnetic domain structures of NiO and other oxide AFM materials such as FeO, CoO, and CuO, and will be important for understanding the magnetic properties of AFM materials, such as the exchange bias effect.

DOI: 10.1103/PhysRevB.85.174401 PACS number(s): 75.60.Ch, 78.70.Dm, 75.50.Ee, 75.80.+q

I. INTRODUCTION

The phenomenon of exchange bias, which arises in a ferromagnetic (FM) layer fabricated on an antiferromagnetic (AFM) substrate, is widely utilized in magnetic storage devices.[1] Despite its technological importance and the amount of time since its discovery,[2] the phenomenon is not yet entirely understood on a microscopic level.[3] Since the magnetic properties at the interface of the system are dependent on the micromagnetic structures (magnetic domain structures) at the surface of the antiferromagnet, detailed investigations of the AFM domain structures are important to understanding the microscopic mechanism of the phenomenon.

NiO is the archetypal AFM material, which has relatively simple AFM domain structures compared to the other antiferromagnets. The Néel temperature is $T_N = 523$ K and it has a collinear spin structure. Owing to the magnetostriction caused by AFM ordering, the NiO crystal below T_N consists of many twinned crystals. The crystallographic twinning leads to four different possible domains, the so-called twin-domains (*T*-domains), with different contractions along the ⟨111⟩ axes. In each *T*-domain three easy spin axes along the ⟨112⟩ directions exist, resulting in the possible three spin domains (*S*-domain) in one *T*-domain. Therefore, in NiO crystal 12 different magnetic domains can exist in total.

The magnetic domain structure can be observed by several kinds of microscopic techniques and has been investigated extensively so far.[4–6] Among these techniques, photoemission electron microscopy (PEEM) combined with x-ray magnetic linear dichroism (XMLD) at the Ni L_2 edge makes the precise observation of *magnetic* *S*-domain structures possible, and the detailed assignment of the magnetic domain contrast to the specific *S*-domain has been reported by comparing the azimuth angle dependence of the observed image contrast with the cluster model calculation including the crystal symmetry and full multiplet splitting.[7]

In addition to the observation by the XMLD effect, even at the O *K* edge, it has been reported by Kinoshita and coworkers that the image contrast can be observed with the *nonmagnetic* x-ray linear dichroic (XLD) effect,[8] and Ohldag and coworkers also have reported the XLD effect in the NiO(100) surface recently.[9] Considering that each O ion is surrounded by six Ni ions whose magnetic moments are antiferromagnetically aligned, the oxygen does not have any magnetic moment. Thus, the observed XLD effect cannot be due to a magnetic effect and the observed image contrast should not be reflecting the magnetic *S*-domain. The observation of simpler domain structures with the XLD effect than with XMLD-PEEM measurements suggests that the XLD-PEEM image contrast reflects the crystallographic *T*-domain structures.[8] The mechanism of the domain observation has been qualitatively discussed as the consequence of the strong interaction between the O 2*p* and Ni 3*d* orbitals and the anisotropy of the O 2*p* orbital.[8,10] The lack of understanding of the observed image contrast by XLD in a *quantitative* manner, however, hampers the assignment of each domain to the specific *T*-domain, as is realized for the *S*-domain investigation by the XMLD effect.[7]

In this paper, we report the precise observation of the azimuth angle dependence (AAD) of the domain contrast by the XLD effect using PEEM at the O *K* edge. Applying both *s*- and *p*-polarized light, it is confirmed that the XLD at the O *K* edge is caused by the x-ray absorption from O 1*s* to the anisotropic O 2*p* orbital that is hybridized with Ni

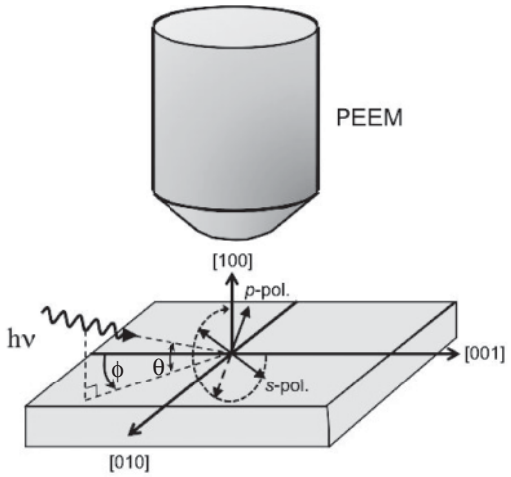

FIG. 1. The experimental geometry of the XLD-PEEM observation at the beamline BL17SU of SPring-8. The angle between the incident light and the sample surface is $\theta = 16^\circ$. The projected components of the propagation vector of the incident light to the surface plane is the [001] direction at the azimuth angle $\phi = 0^\circ$ and the $[0\bar{1}0]$ direction at $\phi = 90^\circ$.

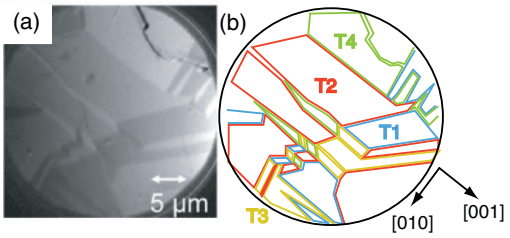

FIG. 2. (Color) (a) Domain structures observed by XLD-PEEM at the O K edge with p-polarized light. Four different XLD contrasts can be seen. (b) Schematic of the domain structures revealed in (a). The four colored solid lines indicate the boundaries of the four types of domains. These correspond to the so-called T-domains of NiO(001) and are labeled as T1, T2, T3, and T4.

$3d$ orbitals. By comparing the AAD of the domain contrast with the calculated AAD of the x-ray absorption cross section with linearly polarized light from the O $1s$ to anisotropic $2p$ orbital one can assign each domain to a specific T-domain in a quantitative manner. The result of the T-domain assignment is in good agreement with the S-domain assignment from a comparison of the AAD of XMLD contrast with a cluster model calculation.[7]

II. EXPERIMENT

The experiments were performed using the PEEM apparatus, SPELEEM (ELMITEC GmbH), installed at the beamline BL17SU of SPring-8. Figure 1 shows the experimental geometry of the PEEM measurement. The angle between the incident soft x-ray and the surface plane is $\theta = 16^\circ$. At the beamline, horizontal and vertical linear polarized light which corresponds to s- and p-polarized light as well as circularly polarized light can be obtained by the multipolarization mode undulator.[11] The projective components of the propagation vector of the incident light to the surface plane of the NiO(100) crystal is the [001] direction at the azimuth angle $\phi = 0^\circ$ and the $[0\bar{1}0]$ direction at $\phi = 90^\circ$. A single-crystal NiO sample was cleaved at the (100) plane in the atmosphere and transferred into the vacuum chamber immediately. More details of the experimental setup are described elsewhere.[7,12]

III. RESULTS AND DISCUSSION

To obtain the angular dependence of the domain contrast by the XLD effect in different domains, we have measured the AAD of XLD images with s- and p-polarized light. Figure 2(a) shows an example of the observed XLD image of NiO(100) taken with p-polarized light at the O K edge. The XLD image is obtained by dividing the image taken at the photon energy of 532.2 eV by that taken at 531.7 eV as in Ref. 7. The way of obtaining the XLD image (i.e., dividing the intensities of the image taken with higher photon energy by that with lower photon energy) is the same as that of obtaining the XMLD image at the Ni L edge in previous studies.[7] As demonstrated in the figure, we can see clear domain contrast by the XLD effect. Four kinds of contrast can be recognized in Fig. 2(a) and the area of the same contrast is color-coded in Fig. 2(b) (blue, red, yellow, and green). As will be discussed in the following section, these four kinds of color-coded areas correspond to the so-called T-domains and are labeled as T1, T2, T3, and T4.

Figures 3(a) and 3(b) show the AAD of XLD contrast of the four types of T-domains with s- and p-polarized light, respectively. When the sample is rotated azimuthally a change of the contrast is clearly seen both in s- and p-polarized light observations. To follow easily the change of the contrast as a function of the angle, some representative domains are fringed and color-coded with the same color as those in Fig. 2(b). The change of the contrast in different azimuth angle ϕ is quite different from the observations with s- and p-polarized light. For example, at $\phi = 0^\circ$ and 87° the difference of the image contrast between different domains is almost zero in (a) s-polarized light observation while the difference is clearly seen in (b) with p-polarized light. In principle, the domain contrast by s-polarized light is simpler than that by p-polarized light. Namely, only two or less contrast variation can be seen in (a). On the contrary, the XLD images by p-polarized light show much richer contrast variation and three or four different contrasts can be seen at -51°, -30°, 30°, 40°, and 60° though only two kinds of contrast are observed at -80° and 0°.

This different domain contrast between s- and p-polarized light observations is intuitively due to the different sensitivity to the in-plane and out-of-plane components between the two. Namely, two T-domains having the same out-of-plane component regarding the contraction axis cannot be distinguished with the s-polarized light observation because of its lack of sensitivity. While the p-polarized light can give different contrasts for the domains because of the different projection of electric field to the contraction axes due to the inclined light incidence. Unlike the x-ray absorption at the Ni $L_{2,3}$ edge, there is no spin-orbit interaction in the final state of x-ray absorption at the O K edge and therefore XLD spectra at the O K edge are not sensitive to the direction of the spin moment at the photoexcited site. Thus, XLD spectra at the O

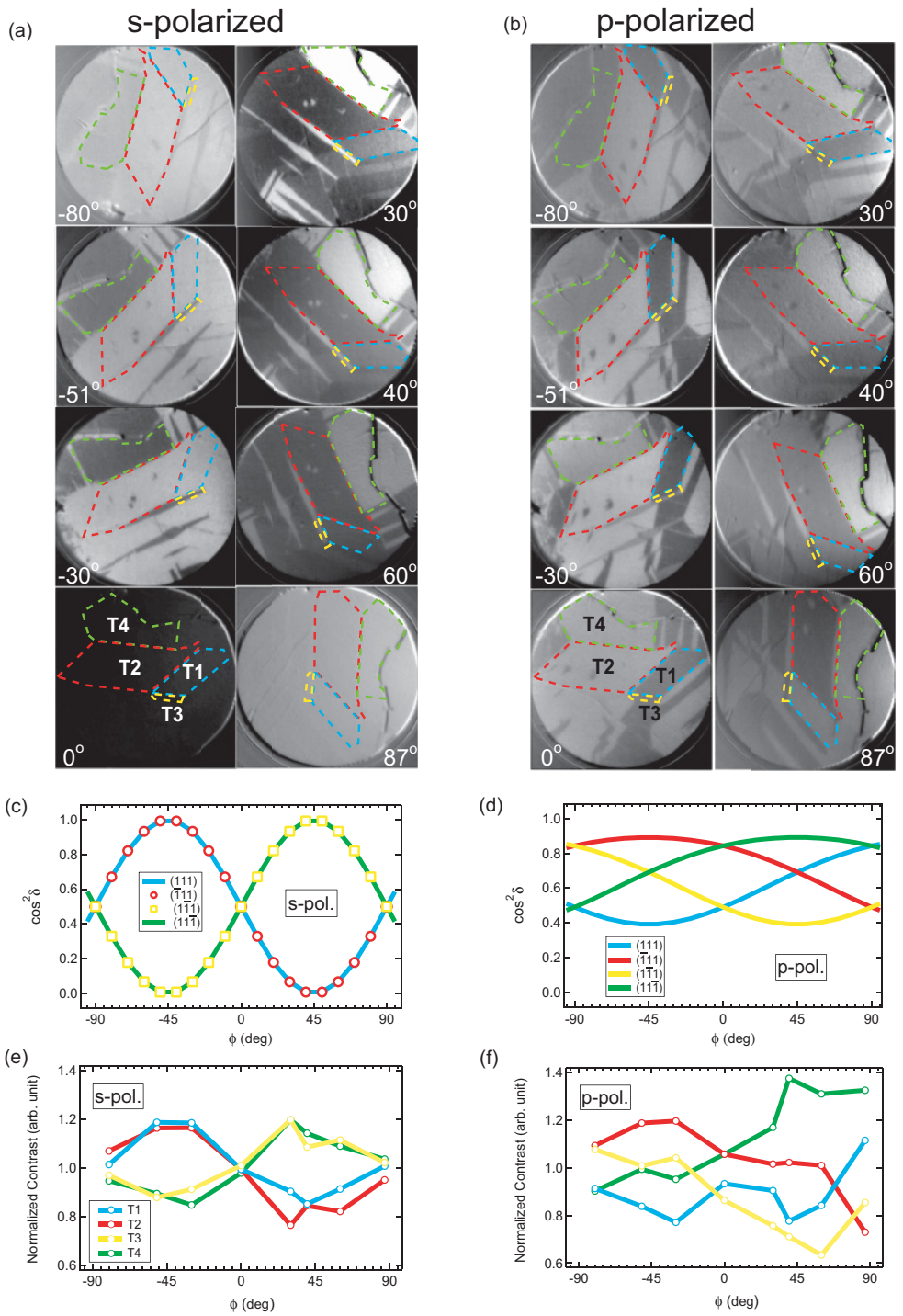

FIG. 3. (Color) Azimuth angle dependence of the XLD domain contrast with (a) s-polarized light and (b) p-polarized light. The angle ϕ is indicated at the corner of each image. The shapes of the representative domains are indicated by dashed lines and labeled tentatively in accordance with Fig. 2(b). The field of view for these XLD images is 30 μm. (c,d) Calculated x-ray absorption intensity as a function of angle ϕ (see Fig. 1) assuming a $\cos^2\delta$ dependence for the O 1s to 2p transition with (c) s-polarized and (d) p-polarized x-ray light. (e,f) Experimentally derived AAD of the contrast of different domains with (e) s-polarized and (f) p-polarized light. The color-coding indicates the different domains following the same scheme as in (a) and (b).

K edge only reflect the symmetry of the spatial wave function. In the presence of AFM order, the point group symmetry of the oxygen site is lowered to the D_{3d} symmetry by the spin alignment of the surrounding Ni sites and the rhombohedral distortion of the lattice due to the magnetostriction. Since no magnetic moment is expected at the oxygen site, the transition matrix of the absorption should be described as a linear combination of the second order invariant tensors of the polarization vector $\mathbf{e}$ under the D_{3d} symmetry operation as $I = A(3\mathbf{e_z}^2 - \mathbf{e}^2) + B\mathbf{e}^2$, where the z axis is chosen to the trigonal axis. From this we immediately obtain the form $I = A'\cos^2\delta + B'$, where δ denotes the angle between the trigonal axis and the polarization vector $\mathbf{e}$ and it is also obvious that the XLD spectra at the O K edge is sensitive only to the T-domains. In contrast, the expression derived in the previous work[7] for the intensity of XLD spectra at the Ni L_2 edge contains spin moments and this shows that the XLD intensity is sensitive to the S-domains at the Ni L_2 edge.

Figures 3(c) and 3(d) show the calculated AAD of x-ray absorption for s- and p-polarized x-ray light (i.e., $\cos^2\delta$ as the function of ϕ where δ is the angle between the polarization vector and the direction of largest amplitude of the final state

$2p$ orbital). Although it is not evident in which direction the $2p$ final state has the largest weight of atomic orbitals in the NiO crystal, it may be along or perpendicular to the $\langle 111 \rangle$ direction if we consider that the crystal contraction of NiO is along the $\langle 111 \rangle$ direction. Here we calculated the AAD, tentatively assuming that the largest weight of atomic $2p$ orbitals is perpendicular to the $\langle 111 \rangle$ (i.e., in the $\{111\}$ plane).

In this assumption the observed AAD of XLD contrast of the domains are in agreement with the calculated AAD of XLD based on the $\cos^2\delta$ relation. For example, the almost zero contrast at $\phi = 0^\circ$ and 87° in s-polarized light observation is well reproduced by the calculation for s-polarized light [Fig. 3(c)] in which every T-domain has the same absorption intensity at 0° and 90°. The simple two-tone contrast at the other azimuth angles is also in good agreement with the calculation in which the absorption intensities are divided into two groups. The observation of a much richer contrast variation with the p-polarized light is also consistent with the calculation for p-polarized light in Fig. 3(d). At $\phi = 0^\circ$ and $\pm 90^\circ$ the x-ray absorption intensities are divided into two groups and at $\phi = \pm 45^\circ$ the variation will be three. In between these special angles the variation can be four.

The agreement between the calculation and the experiment is much more directly confirmed by plotting the value of XLD image intensities as the function of ϕ. Since the brightness of the observed XLD image depends on the experimental conditions (for example, light intensity and inhomogeneous light illumination), to compare the image intensity at different azimuth angle ϕ we have to measure all the images in the same experimental conditions. However, such an experiment is impossible and one cannot directly compare the image intensity.

Nevertheless, if the intensity change follows the trend of the $\cos^2\delta$ dependence, the average absorption intensity should be always constant as in Figs. 3(c) and 3(d). Thus, we have normalized the intensity of the observed domain by the intensity average of all the domains as follows:

$$\tilde{I_{Tn}} = \frac{I_{Tn}}{\left(\sum_{i=1}^{4} I_{Ti}\right)\Big/4}, \quad (n = 1,2,3,4). \tag{1}$$

Here $\tilde{I_{Tn}}$ and I_{Ti} are the normalized and the original intensity of each domain, respectively. We have applied this normalization process in each image in Figs. 3(a) and 3(b) and extract the relative domain intensity of each domain and plot them as the function of the azimuth angle ϕ in Figs. 3(e) and 3(f).

As seen in Figs. 3(e) and 3(f) the observed intensity change of different domains as a function of the angle ϕ is in good agreement with the calculated $\cos^2\delta$ relation both in s- and p-polarized light observations. Especially for the s-polarized light observation, the intensity change almost perfectly coincides with the calculation. The correspondence between the observed intensity change and the calculation for the p-polarized light is not as good as that for the s-polarized light, probably due to the imperfection of the correction of light inhomogeneity or roughness of the sample surface by the normalization procedure. The relative intensity change between different domains, however, almost follows the trend of the $\cos^2\delta$ relation. The agreement between the calculation and the observed AAD of image contrast implies that one can assign each domain to a specific T-domain by comparing the observed AAD with the calculated $\cos^2\delta$ relations. Note that the AAD of XLD domain contrast with s-polarized light is completely the same between the T1 and T2 domains or T3 and T4 domains and one cannot distinguish four different T-domains with s-polarized light observation only. On the other hand, with p-polarized light we can distinguish completely the four different T-domains and the observation of AAD of XLD contrast with p-polarized light is crucial to assign the T-domains completely.

Although the AAD of normalized contrast is in good agreement with the $\cos^2\delta$ relation, there is also a small discrepancy between the two. For instance, we can see three kinds of contrast in Fig. 3(a) [and Fig. 3(e)] at 30° although the $\cos^2\delta$ relation predicts two-tone contrast as in Fig. 3(c). This small discrepancy may be due to a small misalignment between the sample surface and the electric field vector of s-polarized light. By comparing the theoretical curves with experimental ones, however, we can confidently assign the T1, T2, T3, and T4 domains as [111], $[\bar{1}11]$, $[1\bar{1}1]$, and $[11\bar{1}]$ T-domains, respectively. It is worth noting that the assignment of T-domains in this work is consistent with that derived from our previous S-domains assignment in which the AAD of XMLD images were compared with the cluster model calculation.[7] For example, the S-domains inside the T4 domain are assigned as $[\bar{1}21]$, $[2\bar{1}1]$, and [112] by the XMLD measurement in Ref. 7 and these S-domains should be in the $[11\bar{1}]$ plane, consistent with the assigned T-domain by the XLD image with O K edge in the present study.

The validity of the T-domain assignment can also be confirmed by checking the domain wall direction between different T-domains. In Fig. 2(b) we have summarized the assigned T-domain structure of Fig. 2(a). From the illustration we can find that the domain walls between T1 [111] and T2 $[\bar{1}11]$ or T3$[1\bar{1}1]$ and T4 $[11\bar{1}]$ run along the $\langle 011 \rangle$ direction, while the walls between T1 [111] and T3 $[1\bar{1}1]$ or T2 $[\bar{1}11]$ and T4 $[11\bar{1}]$, or T1[111] and T4 $[11\bar{1}]$ run along the $\langle 001 \rangle$ direction. These domain wall directions are consistent with those deduced from the possible boundary structure between each adjacent T-domains as discussed in previous papers.[9,13,14] The consistency of our domain assignment by the XLD of O K edge with those obtained by the XMLD and with the domain wall consideration supports our tentative assumption that the $2p$ final states has a larger weight of atomic orbitals in the $\{111\}$ plane.

Finally, we demonstrate that the T-domain images by XLD can be observed even with circularly polarized light. Figures 4(a), 4(b), 4(c), and 4(d) show the PEEM images of the NiO(100) surface taken at the O K edge with s-, p-, and circularly polarized light, and the sum of images (a) and (b). Because of the richer contrast variation in the p-polarization measurement, some fine structures can be observed in Fig. 4(b) in addition to the relatively simple domain structure observed with the s-polarized light. The sum of the images with s- and p-polarized light results in the very similar image to the observed contrast by the circularly polarized light as compared to Figs. 4(d) and 4(c). Note that the photon energy to obtain the best XLD contrast with circularly polarized light is the

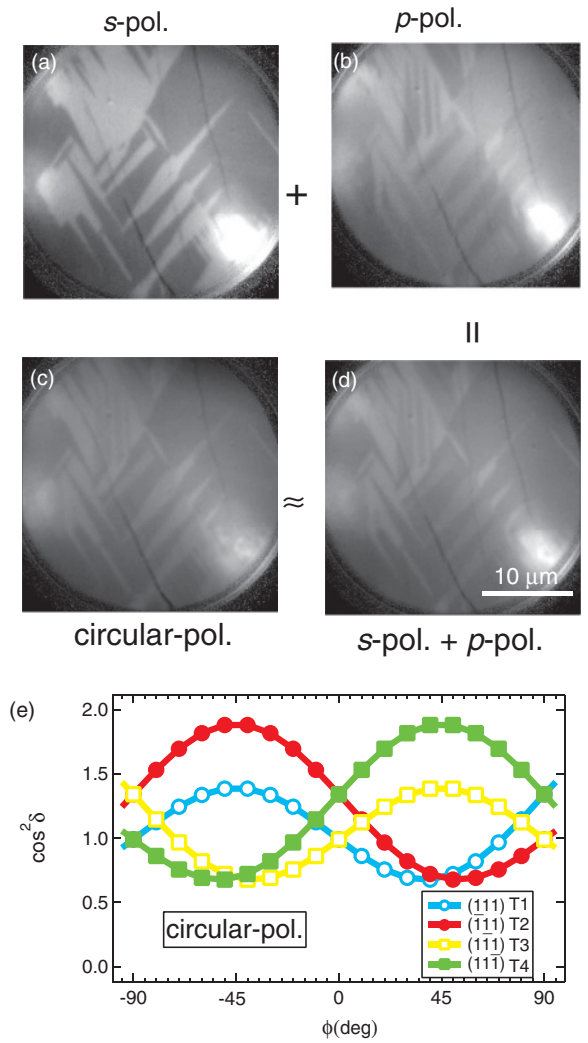

FIG. 4. (Color online) XLD images observed at the O K edge with (a) s-polarized light, (b) p-polarized light, and (c) circularly polarized light. (d) The sum of (a) and (b). The field of view of these images is 30 μm. (e) Calculated AAD of $\cos^2\delta$ for circularly polarized light.

same as that with linearly polarized light ($\sim$ 532.2 eV).[7,9] This good agreement between (c) and (d) arises from the fact that the circularly polarized light is a coherent combination of s- and p-polarized light with $\pi/2$ phase difference each other. Thus, one can obtain both XMLD and XMCD images by using circularly polarized light similarly to the situation that XMLD and XLD images are obtained by unpolarized light[15,16] and successfully applied for the investigation of the magnetic coupling of ferromagnetic film with the antiferromagnetic NiO(001) substrate.[17] Therefore, one can also utilize the XLD image taken with circularly polarized light to distinguish different T-domains. The expected AAD of domain contrast is just a linear combination of those of s- and p-polarized light as indicated in Fig. 4(e). Since every T-domain has different AAD of the XLD contrast one can distinguish four kinds of T-domain with circularly polarized light in principle. The similar sinusoidal pattern between T1 and T2, and T3 and T4, however, may make the identification a little more difficult than that with p-polarized light. On the other hand, utilizing XLD imaging with circularly polarized light for the assignment of a T-domain would be useful for the study of the magnetic properties of a ferromagnetic overlayer on oxide antiferromagnetic materials at the beamlines where one can use only circularly polarized light.

IV. SUMMARY

We have observed the AFM domain contrast of NiO(001) caused by the x-ray linear dichroism at the O K edge by using s- and p-polarized x-rays and a photoemission electron microscope. It is found that the observed azimuth angle dependence of the contrast can be well reproduced by the $\cos^2\delta$ dependency of the x-ray absorption cross section which arises due to the x-ray absorption cross section from the O 1s initial state to an anisotropic 2p final state hybridized with the Ni 3d state. We can unambiguously classify the observed domains into four different T-domains in a quantitative manner by comparing the observed azimuth angle dependence of the domain contrast with the calculation. The results of T-domain assignment are consistent with those derived by the spin-domain assignment in our previous study in which the domain contrast in the x-ray magnetic linear dichroism was compared with a cluster model calculation that included the crystal symmetry and full multiplet splitting. Such domain observations and assignments using a nonmagnetic x-ray linear dichroism can also be anticipated for the family of compounds of NiO such as FeO, CoO, and CuO. This will be helpful in understanding the complicated magnetic domain structure of such materials.

ACKNOWLEDGMENTS

The authors acknowledge the valuable discussions with J. R. Harries. The experiments were performed with the approval of JASRI (Proposals No. 2007A1835, No. 2008A1723, No. 2008A1726, and No. 2009A1667). This research was supported by a Grant-in-Aid for Scientific Research (S, 18101004) from the Japan Society for the Promotion of Science.

*okudat@hiroshima-u.ac.jp

[1] J. Nogues and I. K. Schuller, J. Magn. Magn. Mater. **192**, 203 (1999).
[2] W. H. Meiklejohn and C. P. Bean, Phys. Rev. **102**, 1413 (1956).
[3] K. Fukamichi, A. Sakuma, R. Y. Umetsu, and C. Mitsumata, *Handbook of Magnetic Materials*, edited by K. H. J. Buschow, (Elsevier, New York, 2006), Vol. 16, p. 209.
[4] F. U. Hillebrecht, H. Ohldag, N. B. Weber, C. Bethke, U. Mick, M. Weiss, and J. Bahrdt, Phys. Rev. Lett. **86**, 3419 (2001).
[5] W. L. Roth, J. Appl. Phys. **31**, 2000 (1960).
[6] S. Saito, M. Miura, and K. Kurosawa, J. Phys. C **13**, 1513 (1980).
[7] K. Arai, T. Okuda, A. Tanaka, M. Kotsugi, K. Fukumoto, M. Oura, Y. Senba, H. Ohashi, T. Nakamura, T. Matsushita,

T. Muro, A. Kakizaki, and T. Kinoshita, J. Phys. Soc. Jpn. **79**, 013703 (2010); **79**, 038001 (2010).

[8]T. Kinoshita, T. Wakita, H.-L. Sun, T. Tohyama, A. Harasawa, H. Kiwata, F. U. Hillebrecht, K. Ono, T. Matsushima, M. Oshima, N. Ueno, Y. Saitoh, and T. Okuda, J. Phys. Soc. Jpn. **73**, 2932 (2004).

[9]H. Ohldag, G. van der Laan, and E. Arenholz, Phys. Rev. B **79**, 052403 (2009).

[10]H. Kanda, M. Yoshiya, F. Oba, K. Ogasawara, H. Adachi, and I. Tanaka, Phys. Rev. B **58**, 9693 (1998).

[11]M. Oura, T. Nakamura, T. Takeuchi, Y. Senba, H. Ohashi, K. Shirasawa, T. Tanaka, M. Takeuchi, Y. Furukawa, T. Hirono, T. Ohata, H. Kitamura, and S. Shin, J. Synchrotron Radiat. **14**, 483 (2007).

[12]F. Z. Guo, T. Muro, T. Matsushita, T. Wakita, H. Ohashi, Y. Senba, T. Kinoshita, K. Kobayashi, Y. Saitoh, T. Koshikawa, T. Yasue, M. Oura, T. Takeuchi, and S. Shin, Rev. Sci. Instrum. **78**, 066107 (2007).

[13]W. L. Roth, J. Appl. Phys. **31**, 2000 (1960).

[14]J. N. Armstrong, M. R. Sullivan, and H. D. Chopra, Phys. Rev. B **80**, 104429 (2009).

[15]F. Z. Guo, H. L. Sun, T. Okuda, K. Kobayashi, and T. Kinoshita, Surf. Sci. **601**, 4686 (2007).

[16]G. K. L. Marx, H. J. Elmers, and G. Schönhense, Phys. Rev. Lett. **84**, 5888 (2000).

[17]K. Arai, T. Okuda, A. Tanaka, K. Fukumoto, T. Hasegawa, T. Nakamura, T. Matsushita, T. Muro, A. Kakizaki, and T. Kinoshita, J. Appl. Phys. **110**, 084306 (2011).